

Inversion domain boundaries in ZnO: First-principles total-energy calculations

Yanfa Yan and M. M. Al-Jassim

National Renewable Energy Laboratory, Golden, Colorado 80401, USA

(Received 25 September 2003; published 13 February 2004)

We present first-principles total-energy calculations of domain wall energies for inversion domain boundaries and their interaction with point defects in ZnO. We find that the inversion domain boundaries (IDB's) with Zn-Zn and O-O wrong bonds are energetically unstable, and they transform into the so-called IDB* structures. Although the IDB*'s do not induce electronic states in the bandgap, they are very attractive to electrically active compensating point defects. The segregation of such charged point defects builds up electrical potentials for minority carriers in doped ZnO, which are harmful to optoelectronic applications.

DOI: 10.1103/PhysRevB.69.085204

PACS number(s): 61.72.Nn, 61.72.Yx, 61.72.Ji

Zinc oxide (ZnO) is an important material for next-generation short-wavelength optoelectronic devices such as low-cost light-emitting diodes (LEDs) and laser diodes, transparent *p-n* junctions, large-area flat-panel displays, and solar cells.¹⁻³ In particular, its large exciton binding energy enables optically pumped excitonic lasing at room temperature, and high-temperature emission up to 550 K due to the exciton mechanism.^{4,5} Recently, increasing focus has been directed on the study of ZnO-based electronic device applications.⁶⁻⁸ A prerequisite for such applications is the growth of high-quality *n*- and *p*-type ZnO thin films. However, most ZnO thin films grown on Al₂O₃ or SiC substrates contain a high density of extended defects.⁹ Extended defects are known to play an important role in electronic and mechanical properties of semiconductors. For example, these defects may introduce electrically active energy levels in the energy gap.^{10,11} On the other hand, dopants and impurities may interact with and segregate toward these defects and alter the electronic and structural properties of the material, which can be detrimental under certain conditions. Despite the importance in governing the electronic properties of ZnO thin films, there are very few studies of the atomic structure and effects of the extended defects that may occur in ZnO thin films.

ZnO is similar to GaN in both crystal structure and electronic and optical properties. A recent transmission electron microscopy study revealed that the extended defects in ZnO thin films grown on Al₂O₃ are very similar to the defects found in epitaxial GaN thin films grown on Al₂O₃.⁹ The defects are mainly threading dislocations, stacking faults, and inversion domain boundaries. In GaN, the structure and effects of inversion domain boundaries (IDB's) on the (10 $\bar{1}$ 0) plane have been studied both experimentally and theoretically.^{12,13} The IDB's are found to be inert, i.e., they do not induce electronic levels in the gap. In this paper, we present first-principles total-energy calculations of domain wall energies and the effects for IDB's in ZnO. We find that the IDB's with Zn-Zn and O-O wrong bonds are energetically very unstable. They transform automatically via a translation of $\frac{1}{2}[0001]$ into the so-called IDB* structures, which have no Zn-Zn and O-O wrong bonds. The IDB*'s do not induce electronic structure states in the bandgap, but they are very attractive to electrically active point defects. The

segregation of such charged compensating point defects builds up electrical barriers for minority carriers in both *p*- and *n*-type ZnO, which may be adverse to optoelectronic applications of ZnO.

Our calculations are based on the density-functional theory, using the Vienna *ab-initio* simulation package (VASP).¹⁴ We used the local density approximation for the exchange correlation, and ultrasoft Vanderbilt-type pseudopotentials¹⁵ as supplied by Kresse and Hafner.¹⁶ The Zn 3*d* electrons were treated as part of the valence band. A suitable cutoff energy for the plane-wave basis was determined to be 300 eV. The inversion domain boundaries are modeled with a super cell having two oppositely oriented boundaries in each cell and ten layers of atoms between each boundary. A 40-host-atom supercell was used for domain wall energy calculations. In the calculations of interaction between IDB*'s and point defects, supercells with 160-host atoms were used to avoid the interaction between the point defects themselves. In all defects calculations, all atoms were allowed to relax to reach the minimum energies until the Hellmann-Feynman forces acting on them became less than 0.02 eV/Å.

Structures and energetics. ZnO has wurtzite crystal structure with mixed Zn and O sublattices. The structure of a simple IDB in ZnO is that the occupation of Zn and O sublattices and the Zn-O polarity are reversed across the boundary. Figure 1(a) shows the structure model of a simple IDB for ZnO viewed along the $[11\bar{2}0]$ direction. The Zn and O atoms are interexchanged across the (10 $\bar{1}$ 0) plane. This structure contains the six-membered ring of bonds and each atom is fourfold coordinated, the same as in ZnO bulk. However, the interexchange of Zn and O atoms results in both Zn-Zn and O-O bonds, the so-called wrong bonds. The presence of wrong bonds increases the total energy and thereby reduces the stability of the structure. Northrup *et al.*¹³ found that the IDB shown in Fig. 1(a) transforms via a translation along the $[0001]$ direction into a structure having no wrong bonds. This structure is called IDB*. Figure 1(b) shows the structure of an IDB* in ZnO. This structure contains four-membered rings of bonds, but each atom is fourfold coordinated and there are no Zn-Zn or O-O wrong bonds. The four-membered rings of bonds lead to wrong Zn-O bond angles. Thus, the competition between an IDB and an IDB*

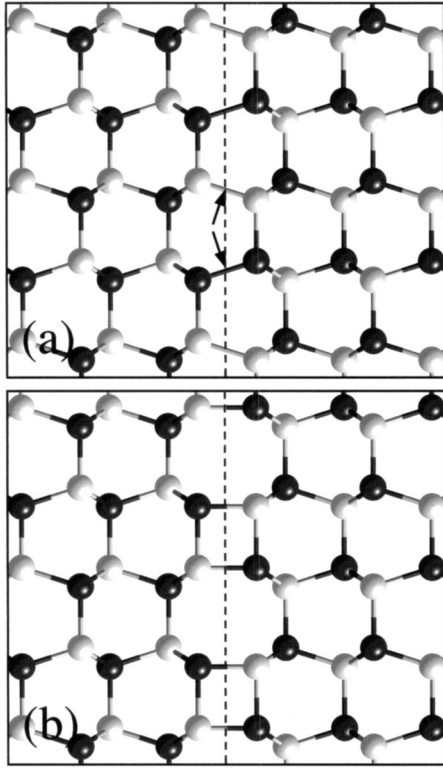


FIG. 1. Structures of (a) a simple IDB and (b) an IDB* in ZnO, viewed along the $[11\bar{2}0]$ zone axis. The boundaries marked by dashed lines are on the $(10\bar{1}0)$ planes. The black arrows indicate the Zn-Zn and O-O wrong bonds.

is the competition between the wrong bonds and wrong bond angles. The result depends highly on the elements forming the compound. An IDB* could be more stable than an IDB in some materials, but it can be opposite in some other materials. Thus, we need to calculate the energetics for both IDB's and IDB*'s in ZnO.

We follow the definition of formation energy for the boundary proposed by Northrup *et al.*¹³ as $E_{\text{form}} = \frac{1}{2}(E - E_{\text{bulk}})$, where E is the total energy of a supercell containing two boundaries and E_{bulk} is the total energy of a reference supercell with bulk structure and with an equivalent number of atoms. In the two total-energy calculations, the cutoff energies were kept the same and the k -point grid was kept equivalent. The domain wall energy σ_{wall} is given by E_{form}/A , where $A = 14.743 \text{ \AA}^2$ is the area of the periodic unit cell of the boundary in the $(10\bar{1}0)$ plane. Our calculation revealed that the simple IDB in ZnO is energetically unstable. It transforms automatically into the IDB* structure via the translation of $\frac{1}{2}[0001]$. This indicates that the Zn-Zn and O-O wrong bonds are energetically very unfavorable.

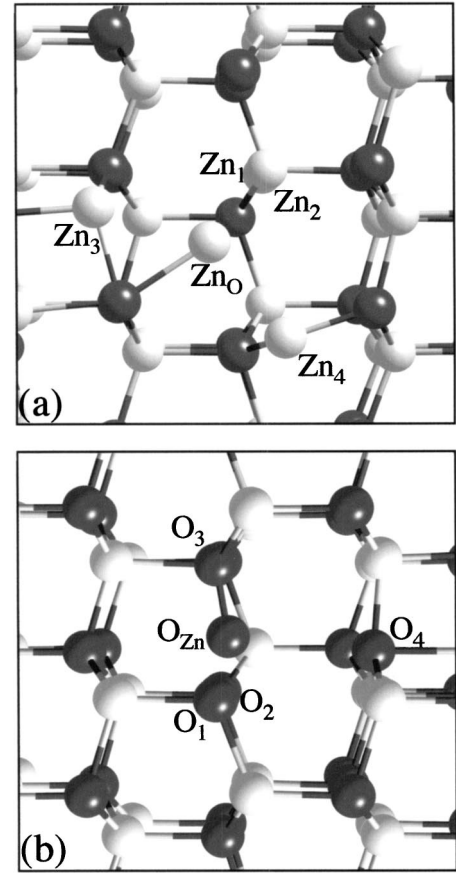


FIG. 2. Structures of fully relaxed (a) Zn_O and (b) O_Zn antisite point defects. The dark balls indicate O atoms, whereas the gray balls are Zn atoms.

This is consistent with the results of Zn_O (a Zn atom occupying an O site) and O_Zn (an O atom occupying a Zn site) antisite defects in bulk ZnO. Figures 2(a) and 2(b) show the structures of calculated fully relaxed Zn_O and O_Zn antisite defects, respectively. The dark balls are O atoms, whereas the gray balls are Zn atoms. We find that Zn atoms do not favor the formation of any Zn-Zn bond. Initially, when a Zn atom replaces an O atom, this Zn atom, the Zn_O in Fig. 2(a), is surrounded by four Zn atoms Zn_1 , Zn_2 , Zn_3 , and Zn_4 , forming four Zn-Zn wrong bonds. After relaxation, the Zn_O atom breaks its initial bonds with its four neighboring Zn atoms and pushes them away. The Zn_O atom also moves toward a nearby O atom and forms a Zn_O -O bond. The bond length of this Zn-O bond is 2.174 Å, about 0.2 Å larger than the bond length of Zn-O in ZnO bulk. For the O_Zn atom, it breaks its three of the four initial bonds with its four surrounding O atoms O_1 , O_2 , O_3 , and O_4 . The O_Zn binds with only one of its four neighboring O atoms, here O_3 , forming

TABLE I. Calculated formation-energy differences of charge neutral point defects at the IDB* and in the crystal-like region in an intrinsic ZnO.

	V_O	V_Zn	Zn_i	O_i	O_Zn	Zn_O	N_O	H_i	Al_Zn	F_O
ΔE_{form}	-0.09	-0.37	-0.60	-0.26	-0.40	-0.24	0.03	-0.38	0.01	-0.13

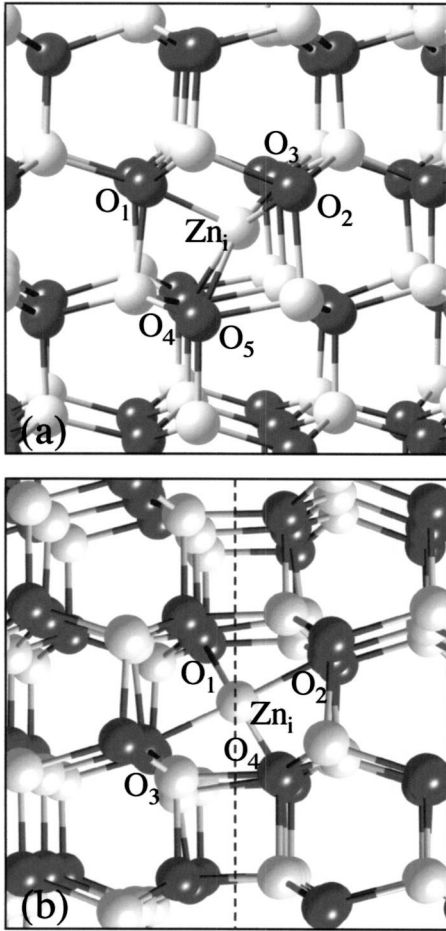


FIG. 3. Structures of fully relaxed Zn_i defects (a) in a ZnO bulk region, (b) at an IDB*. The dark balls indicate O atoms, whereas the gray balls are Zn atoms.

an $O_{Zn}-O_3$ bond. The bond length is 1.461 Å, about 0.22 Å larger than the O-O bond length for an O_2 free molecule. Because of the repulsions between Zn and Zn atoms, and O and O atoms, the simple IDB structure collapses and transforms into the IDB* structure.

The formation energy of an IDB* in ZnO is calculated to be 0.40 eV, which corresponds to a domain wall energy of 27 meV/Å². In the fully relaxed structure, the bond lengths of the Zn-O bond across the boundary is 1.870 Å, which is about 0.1 Å shorter than the bond length of a Zn-O bond in ZnO bulk. This result is probably due to the wrong angle of the Zn-O bonds across the boundary. Calculations of the electronic structure revealed no interface states in the energy region between the valance-band maximum (VBM) and the conduction-band minimum (CBM) for the IDB* structure. This is because gap states typically arise from reduced coordination. However, it does not necessarily mean that an

IDB* in ZnO would not adversely impact the optoelectronic properties of the ZnO thin films, because an IDB* could attract electrically active impurities.

Interaction with impurities. Recently, the effects of extended defects such as stacking faults in semiconductors have received much attention.^{17–20} Because extended defects are very narrow, there is no technique currently available to determine directly the effects of the defects. Most studies were done using theoretical approaches. It is found that although stacking faults in semiconductors do not produce deep levels, they can affect the properties of the host material by interacting with point defects. For example, oxygen impurities tend to segregate toward stacking faults in Si,²¹ because stacking faults act as sinks for point defects. It is also reported that stacking faults in GaAs lower the formation energy of a Si at a Ga site, giving better *n*-type doping.²² However, so far, all reported results indicate that the interaction between stacking faults and impurities is not very strong. The energy difference between an impurity locating on the stacking fault and in a crystal-like region is usually small. This is understandable, because in wurtzite and zinc blende materials, the first-nearest neighbors of an atom at the stacking fault are the same as that of an atom in the perfect-crystal regions, i.e., the tetrahedral symmetry is not altered. Only their second-nearest neighbors are different. When a point defect is introduced, relaxation of surrounding atoms will take place. If the relaxation is small and the symmetry of the first-nearest neighbors is not changed significantly, the relaxation will be similar for the point defect sitting in the crystal-like regions and defects regions. The relaxation caused by a point defect is usually not big enough to change the symmetry significantly of the second-nearest neighbors. Thus, the formation energy of a defect will be similar in the stacking-faults region and in the perfect-crystal region. However, for the IDB*'s, even the first-nearest neighbors of an atom at the boundary are different from those of an atom in the perfect-crystal regions, i.e., the tetrahedral symmetry is altered. The larger open space in the eight-member rings of bonds gives point defects more space to relax. Thus, the IDB*'s may have stronger interaction with point defects than stacking faults.

We investigate the interaction by calculating the formation-energy difference when a point defect is placed in two distinct sites, namely, a defect site and a crystal-like site. The use of the supercell method implies that the point defects are repeated. To avoid the interaction between the point defects themselves, supercells with larger dimensions were constructed. The sampling in the Brillouin zone was performed using the Γ point. Our test calculations revealed that sampling with more *k* points does not change the relative energies. The formation-energy difference is obtained as

TABLE II. Calculated formation-energy differences of charge point defects at the IDB* and in the crystal-like region in a *p*-type ZnO.

	V_O^{+1}	V_O^{+2}	Zn_i^{+1}	Zn_i^{+2}	O_i^{+1}	O_i^{+2}	O_{Zn}^{+1}	O_{Zn}^{+2}	Zn_O^{+1}	Zn_O^{+2}	H_i^{+1}	N_O^{-1}
ΔE_{form}	-0.20	-0.30	-0.64	-0.77	-0.20	-0.23	-0.39	-0.44	-0.27	-0.55	-0.14	0.11

TABLE III. Calculated formation-energy differences of charge point defects at the IDB* and in the crystal-like region in an *n*-type ZnO.

	V_{Zn}^{-1}	V_{Zn}^{-2}	O_{Zn}^{-1}	O_{Zn}^{-2}	$\text{Al}_{\text{Zn}}^{+1}$	F_{O}^{+1}
ΔE_{form}	-0.36	-0.44	-0.09	-0.15	0.01	-0.16

$$\Delta E_{\text{form}} = E_{\text{tot}}(\text{IDB}^*) - E_{\text{tot}}(\text{CL}), \quad (1)$$

where $E_{\text{tot}}(\text{IDB}^*)$ is the total energy of a supercell with the point defect placed in the IDB*, and $E_{\text{tot}}(\text{CL})$ is the total energy of the same supercell with the point defect placed in crystal-like region.

Native defects such as V_{Zn} , V_{O} (vacancies), Zn_i , O_i (self-interstitials), Zn_{O} and O_{Zn} (antisites) play important roles in determine the electronic properties of ZnO film. For example, Zn_i , O_i , V_{O} , and Zn_{O} are “donorlike” defects and can compensate acceptors, which are detrimental to the *p*-type doping of ZnO. On the other hand, V_{Zn} and O_{Zn} are “donor killer” defects, which are detrimental to the *n*-type doping of ZnO. For *p*-type doping of ZnO, so far the best dopant is found to be N.²³ For *n*-type doping of ZnO, Al, and F have been proven to be good dopants.^{24,25} H atoms are also found to be donors in ZnO, and they are often incorporated unintentionally in ZnO.²⁶ Thus, we investigate the interaction between the IDB*’s and the native defects, such as V_{O} , V_{Zn} , Zn_i , O_i , Zn_{O} , and O_{Zn} and dopant impurities such as N, Al, F, and H.

Table I shows the calculated energy differences for the defects in their neutral charge state. The results show that the IDB* lowers significantly the formation energies of V_{Zn} , Zn_i , O_{Zn} , Zn_{O} , and H, whereas it has very little interaction with the dopant impurities such as N, Al, and F. In particular, the formation energy of a Zn_i at the IDB* decreases 0.60 eV with respect to that in a crystal-like site. This large difference in the formation energy can be explained by the local structure close to the IDB*. Figures 3(a) and 3(b) show side views of relaxed structures for a Zn_i in a crystal-like region and at an IDB*, respectively. In the crystal-like region, the Zn_i atom binds with five surrounding O atoms, marked by O_1 , O_2 , O_3 , O_4 , and O_5 in Fig. 3(a), forming five Zn-O bonds. Thus, the Zn_i atom is *not* fourfold coordinated, which is different from that in the crystal-like regions. At the IDB*, indicated by the dashed line in Fig. 3(b), because of the eight-member ring of bonds, the Zn_i atom only binds with four O atoms O_1 , O_2 , O_3 , and O_4 . Thus, the Zn_i atom remains fourfold coordinated, the same as that in the crystal-like regions. Thus, a Zn_i atom locating at the IDB* is energetically more favorable than locating in a crystal-like region.

Effects. The point defects with neutral charge states are usually not harmful to the electronic properties of most semiconductors, unless they are charged. Thus we also investigated the interaction between the IDB* and the above point defects with various charged states. In *p*-type ZnO, the positively charged defects are important, because they compensate the acceptors. The possible positively charged point defects include V_{O}^{+1} , V_{O}^{+2} , Zn_i^{+1} , Zn_i^{+2} , O_i^{+1} , O_i^{+2} ,

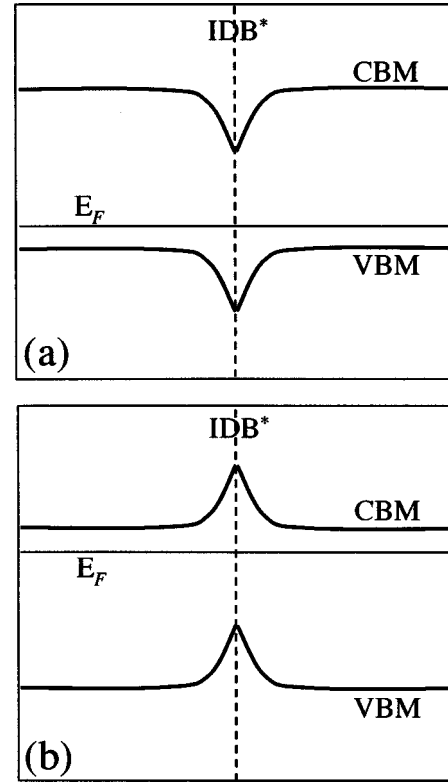


FIG. 4. The segregation of charged compensating defects at the IDB* sets up a *p-i-p* band structure in *p*-type ZnO and an *n-i-n* band structure in *n*-type ZnO.

$\text{O}_{\text{Zn}}^{+1}$, $\text{O}_{\text{Zn}}^{+2}$, $\text{Zn}_{\text{O}}^{+1}$, and $\text{Zn}_{\text{O}}^{+2}$, and H^{+1} . Table II gives the calculated formation-energy differences for these charged defects. For comparison, the calculated formation-energy difference for ionized dopant N^{-1} is also given. The results show that the IDB* lowers significantly the formation energies of all positively charged point defects, whereas it increases the formation-energy of ionized N dopant. In *n*-type ZnO, the negatively charged point defects are important, because they are the electron killers. The possible negatively charged point defects are V_{Zn}^{-1} , V_{Zn}^{-2} , $\text{O}_{\text{Zn}}^{-1}$, and $\text{O}_{\text{Zn}}^{-2}$. Table III gives the calculated formation-energy differences for these charged defects. For comparison, the calculated formation-energy differences for ionized *n*-type dopants Al^{+1} and F^{+1} are also shown. The results show that the IDB* lowers significantly the formation energies of all negatively charged point defects, whereas it has very little effect on the charged dopant impurities.

It is clear from the above calculation that in both *p*- and *n*-type ZnO, the IDB*’s are attractive to the charged compensating point defects. The concentration of these compensating defects will be much higher at the boundary than in the perfect-crystal regions. These excess charged defects will set up a space-charged region at both sides of the boundary, and bend the conduction and valence bands, forming a *p-i-p* junction in *p*-type ZnO and an *n-i-n* junction in *n*-type ZnO, as shown in Fig. 4, where the dashed lines indicate the positions of the IDB*’s. These junctions are electrical potentials to the minority carriers. Thus, they are deleterious to the optoelectronic applications of ZnO.

In conclusion, we have presented first-principles total-energy calculations of domain wall energies for IDB's and their interaction with point defects. We found that the Zn-Zn and O-O wrong bonds are very unfavorable energetically in ZnO. Thus, the IDB's with Zn-Zn and O-O wrong bonds are unstable, and they transform automatically via a translation of $\frac{1}{2}[0001]$ into the so-called IDB* structures, which have no Zn-Zn and O-O wrong bonds. Although the IDB*'s do not induce electronic structure states in the bandgap, they are very attractive to electrically active point defects. The segregation of such charged compensating point defects builds up electrical potentials for minority carriers in both *p*- and

n-type doped ZnO. Thus, the IDB*'s should have an adverse impact on optoelectronic applications of ZnO.

The *ab initio* total-energy and molecular dynamics package, Vienna *ab initio* simulation package (VASP), was developed at the Institute für Theoretische Physik of the Technische Universität Wien. This research was supported by the U.S. Department of Energy under Contract No. DE-AC36-99GO10337, and used resources of the National Energy Research Scientific Computing Center, which is supported by the Office of Science of the U.S. Department of Energy under Contract No. DE-AC03-76SF00098.

-
- ¹J. R. Tuttle, M. A. Contreras, T. J. Gillespie, K. R. Ramanathan, A. L. Tennant, J. Keane, A. M. Gabor, and R. Noufi, *Prog. Photovoltaics Res. Appl.* **3**, 235 (1995).
- ²H. J. Ko, Y. F. Chien, S. K. Hong, H. Wensch, T. Yao, and D. C. Look, *Appl. Phys. Lett.* **77**, 3761 (2000).
- ³X. L. Guo, J. H. Choi, H. Tabata, and T. Kawai, *Jpn. J. Appl. Phys.* **40**, L177 (2001).
- ⁴Y. Segawa, A. Ohtomo, M. Kawasaki, H. Koinuma, Z. K. Tang, P. Yu, and G. K. L. Wong, *Phys. Status Solidi B* **202**, 669 (1997).
- ⁵D. M. Bagnall, Y. F. Chen, Z. Zhu, T. Yao, M. Y. Shen, and T. Goto, *Appl. Phys. Lett.* **73**, 1038 (1998).
- ⁶R. L. Hoffman, B. J. Norris, and J. F. Wager, *Appl. Phys. Lett.* **82**, 733 (2003).
- ⁷Y. R. Ryu, S. T. Lee, and H. W. White, *Appl. Phys. Lett.* **83**, 87 (2003).
- ⁸H. Ohta, H. Mizoguchi, M. Hirano, S. Narushima, T. Kamiya, and H. Hosono, *Appl. Phys. Lett.* **82**, 823 (2003).
- ⁹D. Gerthsen, D. Litvinov, Th. Gruber, C. Kirchner, and A. Waag, *Appl. Phys. Lett.* **81**, 3972 (2002).
- ¹⁰H. Iwata, U. Lindefelt, S. Oberg, and P. R. Briddon, *Phys. Rev. B* **65**, 033203 (2003).
- ¹¹H. Iwata, U. Lindefelt, S. Oberg, and P. R. Briddon, *J. Appl. Phys.* **93**, 1577 (2003).
- ¹²L. T. Romano, J. E. Northrup, and M. A. O'Keefe, *Appl. Phys. Lett.* **69**, 2394 (1996).
- ¹³J. E. Northrup, J. Neugebauer, and L. T. Romano, *Phys. Rev. Lett.* **77**, 103 (1996).
- ¹⁴G. Kresse and J. Hafner, *Phys. Rev. B* **47**, 558 (1993); **49**, 14 251 (1994); G. Kresse and J. Furthmüller, *ibid.* **54**, 11 169 (1996).
- ¹⁵D. Vanderbilt, *Phys. Rev. B* **41**, 7892 (1990).
- ¹⁶G. Kresse and J. Hafner, *J. Phys.: Condens. Matter* **6**, 8245 (1994).
- ¹⁷A. Antonelli, J. F. Justo, and A. Fazzio, *Phys. Rev. B* **60**, 4711 (1999).
- ¹⁸Y. Yan, M. M. Al-Jassim, and T. Demuth, *J. Appl. Phys.* **90**, 3952 (2001).
- ¹⁹T. M. Schmidt, R. H. Miwa, W. Orellana, and H. Chacham, *Phys. Rev. B* **65**, 033205 (2002).
- ²⁰R. H. Miwa, P. Venezuela, and A. Fazzio, *Phys. Rev. B* **67**, 205317 (2003).
- ²¹S. Senkader, J. Esfandyari, and G. Hobler, *J. Appl. Phys.* **78**, 6469 (1999).
- ²²T. M. Schmidt, J. F. Justo, and A. Fazzio, *Appl. Phys. Lett.* **78**, 907 (2001).
- ²³M. Joseph, H. Tabata, and T. Kawai, *Jpn. J. Appl. Phys.* **38**, 1205 (1999).
- ²⁴A. A. Singh and R. M. Mehra, *J. Appl. Phys.* **90**, 5661 (2001).
- ²⁵T. Miyata, S. Ida, and T. Minami, *J. Vac. Sci. Technol. A* **21**, 1404 (2003).
- ²⁶C. G. Van de Walle, *Phys. Rev. Lett.* **85**, 1012 (2000).